Structural Engineering and Mechanics, Vol. 40, No. 4 (2011) 517-539
DOI: http://dx.doi.org/10.12989/sem.2011.40.4.517

Shake-table responses of a low-rise RC building model having irregularities at first story

Han Seon Lee*[1], Dong Wook Jung[2], Kyung Bo Lee[1], Hee Cheul Kim[3] and Kihak Lee[4]

[1]*School of Civil, Environmental, and Architectural Engineering, Korea University, Seoul 136-713, Korea*
[2]*Structural Engineer, OPUS PEARL Co., Seoul 135-811, Korea*
[3]*Department of Architectural Engineering, Kyunghee University, Kyunggido 447-701, Korea*
[4]*Department of Architectural Engineering, Sejong University, Seoul 143-747, Korea*

(Received February 8, 2011, Revised June 15, 2011, Accepted October 11, 2011)

Abstract. This paper presents the seismic responses of a 1:5-scale five-story reinforced concrete building model, which represents a residential apartment building that has a high irregularity of weak story, soft story, and torsion simultaneously at the ground story. The model was subjected to a series of uni- and bi-directional earthquake simulation tests. Analysis of the test results leads to the following conclusions: (1) The model survived the table excitations simulating the design earthquake with the PGA of 0.187 g without any significant damages, though it was not designed against earthquakes; (2) The fundamental mode was the torsion mode. The second and third orthogonal translational modes acted independently while the torsion mode showed a strong correlation with the predominant translational mode; (3) After a significant excursion into inelastic behavior, this correlation disappeared and the maximum torsion and torsion deformation remained almost constant regardless of the intensity of the two orthogonal excitations; And, (4) the lateral resistance and stiffness of the critical columns and wall increased or decreased significantly with the large variation of acting axial forces caused by the high bi-directional overturning moments and rocking phenomena under the bi-directional excitations.

Keywords: earthquake simulation test; irregularity; reinforced concrete; torsion; bi-directional excitation

1. Introduction

Many low-rise residential apartment buildings have recently been constructed in the densely populated areas of Korea. As a result of the lack of available sites, the ground floor is used for a parking lot and a piloti story is adopted. This type of buildings as shown in Fig. 1(a), commonly has a high irregularity of soft story, weak story, and torsion simultaneously at the ground story. Observations of the damages to the structures imposed by the severe earthquakes, such as the 1995 Kobe (Fukuta *et al.* 2001) and 2008 Sichuan earthquakes (Zhao *et al.* 2009), have drawn the conclusion that this type of building structures are vulnerable to severe damages or complete collapse of the ground story. A large number of these buildings have been constructed without considering earthquake resistant design requirements in Korea. However, the new Korean Building Code (KBC) 2005 (Architectural Institute of Korea 2005), which basically follows the framework of

*Corresponding author, Professor, E-mail: hslee@korea.ac.kr

the International Building Code (IBC) 2000 (International Code Council 2000) with some minor modifications, and the other related building laws enforce the seismic design of these building structures. Retrofitting the existing building structures has been one of the main research topics, worldwide, since the 1990's. Particularly, the advancement in performance-based seismic evaluation technique such as FEMA 356 (FEMA 2000) and ASCE-SEI 41 (American Society of Civil Engineers 2006) has made the application of retrofitting to general building structures possible. Nevertheless, the information available in these recommendations is still not sufficient to cover all types of building structures, particularly highly irregular structures, and more experimental and analytical elaborations are needed.

The former studies on the seismic performance of the gravity-load designed (GLD) RC structures were mainly addressed for the bare moment-resisting plane frames or masonry-infilled plane frames subjected to uni-directional seismic excitations (Bracci *et al*. 2001, Lee and Woo 2002, Hashemi and Mosalam 2006, Wu *et al*. 2009) However, the effect of the ground motions in the orthogonal direction on the global and local responses of the structures can be significant in the case of reinforced concrete structures (Hosoya *et al*. 1995). Furthermore, the seismic responses of three-dimensional high-rise structures having high degrees of irregularity such as weak/soft story and torsion eccentricity can be much more complicated (Ko and Lee 2006). Through pseudo-dynamic tests, European researchers have studied the seismic behaviors of RC three-dimensional structures having irregularities with and without masonry infill (Bousias *et al*. 2007, Di Ludovico *et al*. 2008).

The research presented herein aims at the investigation of realistic seismic responses of a low-rise RC building structure having high degrees of irregularity in weak/soft story and torsion at the ground story through shake-table earthquake simulation tests both in one direction and in two orthogonal directions. The validity of KBC 2005 (IBC 2000) for the seismic design and evaluation of this highly irregular building structure will be evaluated. The seismic performance of the building structure will then be checked by applying FEMA356 assessment models to the test results.

2. Design and construction of the model

The prototype was determined based on the inventory study (Lee 2010) and designed by considering the gravity loads only. Drawings of the prototype are shown in Figs. 2(a), (b), and (c). The reinforcement details are non-seismic details according to the construction practice in Korea and the details of main members at the ground story are given in Figs. 2(d) and (e). According to KBC2005, the design earthquake is defined as the level of two thirds of the intensity of earthquake

(a) An example in Korea (b) Overview of the model and experimental setup

Fig. 1 Low-rise residential building and model

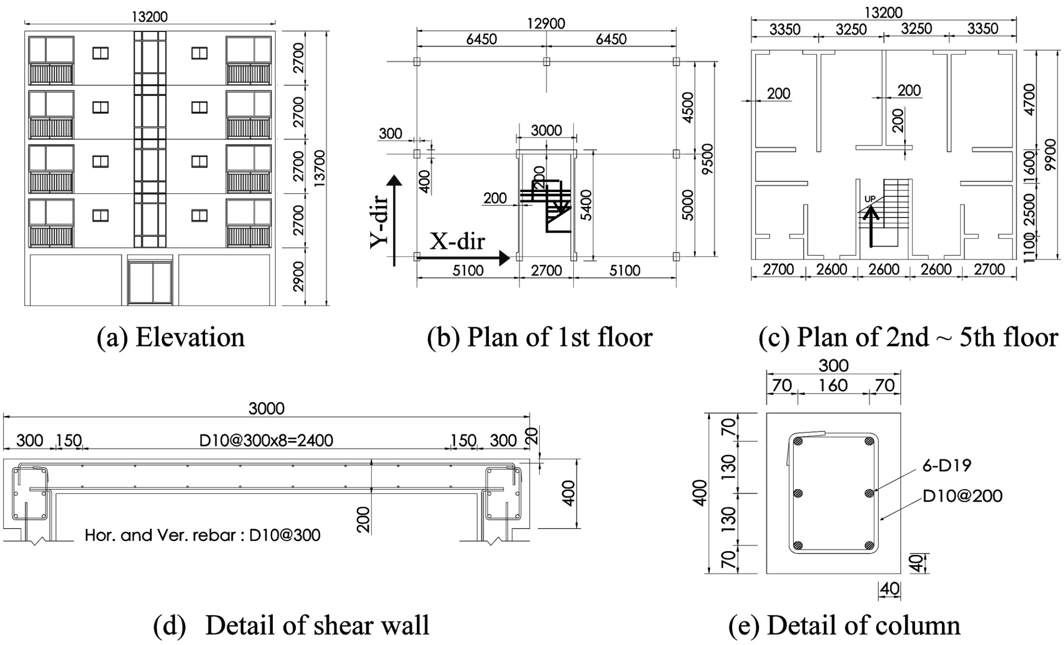

Fig. 2 Prototype structure (unit: mm)

ground motions with the return period of 2500 years in Korea. With the assumption of soil type, Sc, the earthquake load for the prototype is introduced for reference as follows according to KBC 2005, although it was not designed for this load

$$V = C_s \cdot W = 0.176 \times 7147 = 1258 \text{ kN} \tag{1}$$

$$C_s = \frac{S_{D1}}{(R/I_E)T} = \frac{0.2341}{(3/1.2)0.348} = 0.269 \text{, but, not exceeding } C_S = \frac{S_{DS}}{R/I_E} = \frac{0.439}{(3/1.2)} = 0.176 \tag{2}$$

$$T = 0.049(h_n)^{3/4} = 0.049 \times 13.7^{3/4} = 0.348 \text{ s} \tag{3}$$

where, V: base shear, C_s: seismic coefficient, W: effective seismic weight, R: response modification factor, T: fundamental period (sec), h_n: height of structure (m), S_{D1}, S_{DS}: spectral accelerations at period 1sec and 0.2 sec, respectively, I_E: importance factor.

The evaluations of the prototype regarding the irregularities in accordance with KBC 2005 are given in Table 1. Strength and torsion irregularities in particular appear to be very high.

Table 1 Assessment of irregularity at first story according to KBC2005

Irregularity	Criteria	*X*-dir.	*Y*-dir.
Stiffness	$^*k_1/k_2 < 0.7$	582 / 931 = 0.63 < 0.7	1507 / 2284 = 0.66 < 0.7
Strength	$^{**}F_1/F_2 < 0.8$	1.92 / 4.18 = 0.46 < 0.8	3.48 / 8.39 = 0.42 < 0.8
Torsion	$^{\S}\delta_{max}/\delta_{avg} > 1.2$	5.94 / 4.22 = 1.41 > 1.2	2.8 / 1.2=2.34 > 1.2

$^*k$: story stiffness, $^{**}F$: strength, 1, 2: story number, $^{\S}\delta_{max}$, δ_{avg}: maximum and average drift.

A 1:5 scale model was determined considering the capacity of the available shaking table at the Korea Institute of Machinery and Material (KIMM), which is 4 m × 4 m in size, with the pay load capacity of 300 kN and the six-degree-of-freedom control. The relationship between stress and strain of the model materials was assumed to satisfy the requirements of the true replica model (Harris and Sabnis 1999). The associated ratios of length, mass, force and time of the model with respect to the full scale are shown in Table 2. The portion of the lowest two stories was constructed to strictly satisfy the similitude requirements, while the portion of the upper three stories was replaced by the concrete blocks of similar volume. These blocks were again separated into three piers connected at the top with L-Shape steel beams in order to distribute the gravity load and supply the lateral stiffness appropriately. This modified model enabled the reduction of time and cost for construction without significant loss of similitude in the response. The total mass of the

Table 2 Similitude law

Item	Dimension	True replica model	Item	Dimension	True replica model
Length, l	L	1/5	Acceleration, $\ddot{x}$	LT^{-2}	1
Area, A	L^2	1/25	Strain, ε	-	1
Mass, M	M	1/25	Stress, σ	FL^{-2}	1
Force, F	MLR^{-2}	1/25	Time(period), t	T	$1/\sqrt{5}$

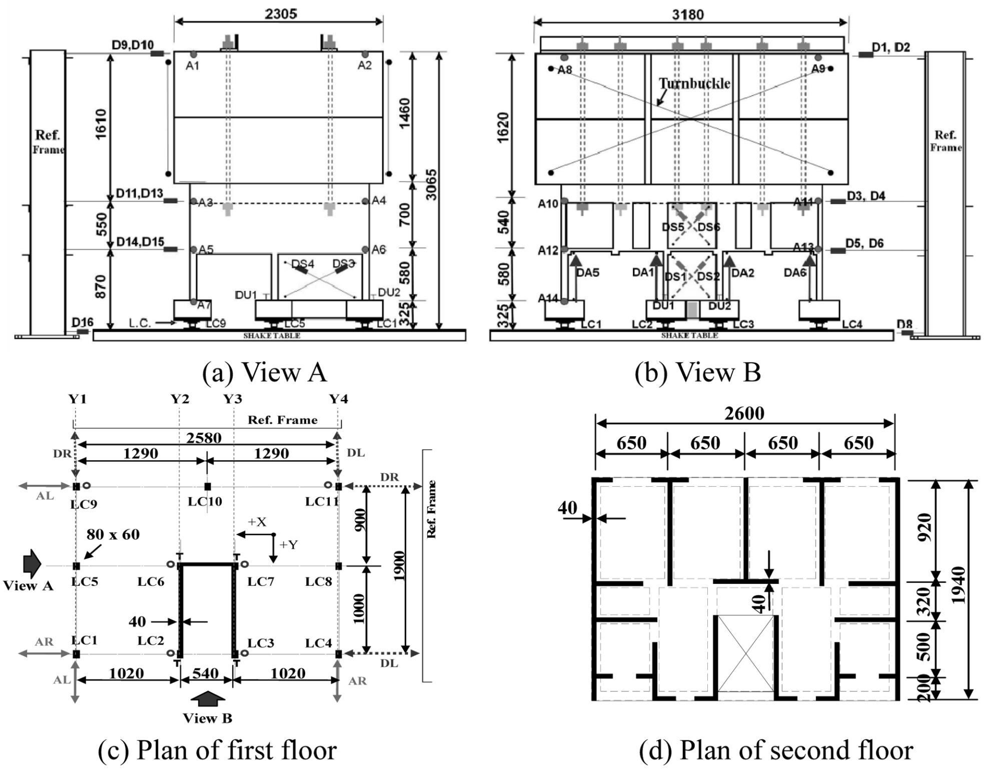

(a) View A (b) View B

(c) Plan of first floor (d) Plan of second floor

Fig. 3 Dimensions of the model and instrumentation (unit: mm)

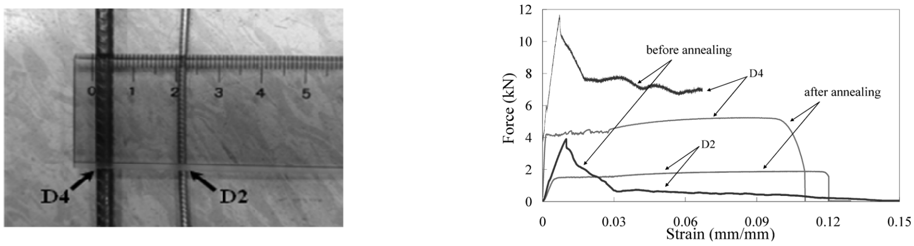

(a) D2 and D4 Rebar (b) Typical force versus strain relation

Fig. 4 Model reinforcement D2 and D4

model is estimated to be 265.9 kN, which is 7% less than the 285.9 kN required by the similitude for the true replica model.

Dimensions and details of the model are shown in Fig. 3. The maximum size of coarse aggregate in model concrete was limited to 4 mm. Since it was difficult to make the cross sections of the model reinforcement conform exactly to the similitude law, the yield forces rather than yield stresses were selected as the target (Lee and Woo 1998). The model reinforcements, D4 and D2, representing the D19 and D10 reinforcements with the nominal yield strength of 400 MPa (in prototype), were made by deforming wires.

Heat treatment was conducted on these model reinforcements to ensure the target yield forces (D4: 4.4 kN, D2: 1.1 kN) in accordance with the similitude requirements. The model reinforcements and typical results of tension tests are shown in Fig. 4. The achieved average yield forces of model reinforcements, D4 and D2, were 4.56 kN and 1.3 kN, respectively. The average compressive strength of the model concrete obtained from 28-day compressive cylinder tests was 30.2 MPa with the design strength of 21 MPa.

3. Experimental setup, instrumentation and test program

The experimental set-up and instrumentation to measure the displacements, accelerations, and forces are shown in Fig. 3. The drifts and accelerations were measured in two orthogonal directions at the right and left side from each view point. The load cells were installed beneath the footings to measure the two orthogonal shear forces and the axial forces (Kang 2004). The reference frames to measure the lateral displacement of the model and shake table were set up outside the shaking table. Instrumentation to measure shear deformation of the walls and the uplift and elongations of the columns are also shown. The overview of the model and experimental set-up is given in Fig. 1(b). The final values of axial forces measured at the load cells after the concrete blocks were attached on top of the third floor are shown in Table 3. Since load cells LC2 and LC3 did not function well, the corresponding data were excluded.

The program of earthquake simulation tests is summarized in Table 4. The target or input

Table 3 Measured axial forces after attachment of concrete blocks (unit: kN)

Load cell	LC1	LC4	LC5	LC6	LC7	LC8	LC9	LC10	LC11	Sum
Axial force	16.6	1.1	8.9	91.6	65.8	6.1	16.9	11.2	3.6	239.9

Table 4 Test program (*X*-dir: Taft N21E, *Y*-dir: Taft S69E)

Test Designation	Intended PGA (g)		Measured PGA (g)		Remark (Earthquake in Korea)
	X-dir.	*Y*-dir.	*X*-dir.	*Y*-dir.	
0.035 *X*	0.035	-	-	-	-
0.035 *XY*	0.035	0.040	-	-	
0.070 *X*	0.070	-	0.076	-	Return period (50yr)
0.070 *XY*	0.070	0.080	0.075	0.145	
0.154 *X*	0.154	-	0.185	-	Return period (500yr)
0.154 *XY*	0.154	0.177	0.210	0.289	
0.187 *X*	0.187	-	0.209	-	Design earthquake,
0.187 *XY*	0.187	0.215	0.268	0.284	(2/3 × intensity of the earthquake with the return period of 2500 years)

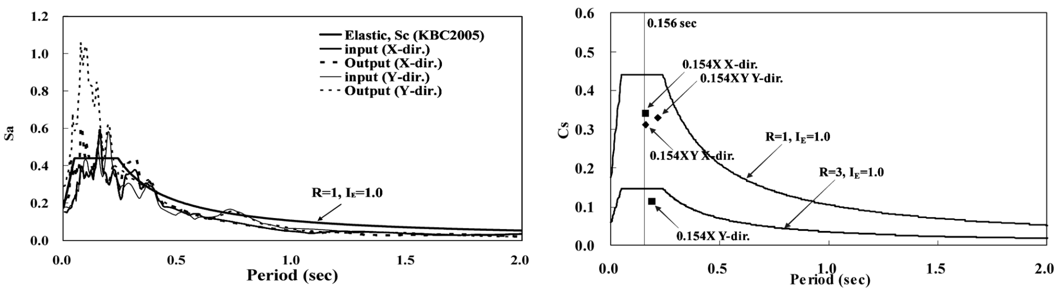

(a) Elastic design and response spectra (b) Test results with the design spectra

Fig. 5 KBC 2005 design and output response spectra (Period axis compressed by $1/\sqrt{5}$)

accelerogram of the table was based on the recorded 1952 Taft N21E (*X* direction) and Taft S69E (*Y* direction) components, and was formulated by compressing the time axis with the scale factor of $1/\sqrt{5}$ and by adjusting the peak ground acceleration (PGA) to match the corresponding (KBC2005) elastic design spectrum. The designation and significance of each earthquake simulation test are given in the table. First, the test was performed with the table excitations in only one direction (*X* direction), and the consecutive test was then conducted in the two orthogonal directions (*X* and *Y* directions) for each level of earthquake intensity. Detailed information on the design, construction, the tests of this model and the test results can be found in reference (Jung 2010).

4. Test results and observations

Because the shaking table has not been maintained well and bi-direction tests were rarely conducted before these tests, the table did not function as directed by the computer input. The measured shake table output was much higher in the *Y* direction than the intended input as given in Table 4. As a result, since the output of 0.154*XY* appear to be similar to the input of 0.187*XY* originally intended for the design earthquake and the response spectra of these output in Fig. 5(a) generally simulate the design spectrum, the response of the model under test 0.154*XY* is assumed to represent the response of the model to the design earthquake, though the intensity of excitation in the *Y* direction, 0.289 g, still significantly exceeded the intended value, 0.215 g, in test 0.187*XY*. Also, the response spectrum to this output in Fig. 5(a) appears to be almost two times larger than the design spectrum in the short period range.

Analysis will be performed mainly on the responses of the model under test 0.154*XY* which represents the design earthquakes in Korea. However, one of the main aspects to be observed in this research is the effect of the bi-directional excitations in comparison with the uni-directional. Therefore, the responses of the model under the uni-directional excitation in the *X* direction, 0.154*X*, will be investigated and compared with those of 0.154*XY*. Additionally, since the response of the model revealed relatively large inelastic responses under test 0.154*XY*, the responses of the model under test 0.070*XY* will be observed as representative of the elastic response characteristics.

4.1 Global responses

General trends in drift and acceleration histories under 0.154*XY*: Time histories of drifts and accelerations at the level of the second and third floors and the roof under the 0.154*XY* test, are shown in Fig. 6. The locations of measurements defined in Figs. 3(a) and (b) are denoted as the right and left sides for the drifts (DR and DL) and accelerations (AR and AL) in the opposite way depending on the viewpoint in Fig. 3(c). The maximum values of responses on the positive and negative sides are given with the corresponding time instants in Fig. 6, and likewise in the following Figs. 7, 8 and 9. Though the model is symmetric along the *Y* direction, the right side showed larger drifts than the left side, which means the larger accelerations on the left side than on the right side. It can be noted in Figs. 6(a) to (d) that the concrete blocks behaved not as a rigid body but as a deformable body by showing larger roof drifts than the drifts at the third level. It can be further found that the maximum positive and negative values of drift and acceleration in the *Y* direction are in general larger than those in the *X* direction. Inertia forces of the model were derived by assuming the linear distribution of acceleration between the measured accelerations in Figs. 6(e) to (h). Inertia torsion and torsion deformation were calculated by averaging the corresponding values in the *X* and *Y* directions. It should be noted that since the vertical accelerations were not measured, the inertia overturning moments were derived by using measured horizontal accelerations only.

Comparison of global responses derived from inertia forces versus load cells: The time histories of story drifts, base shears and overturning moments in the *X* and *Y* directions, and torsion moment and torsion deformation at the first story are given in Fig. 7, Fig. 8, and Fig. 9, for 0.154*XY*, 0.154*X*, and 0.070*XY*, respectively. The time histories of the base shears, overturning moments, and torsion moment derived from load cells are superposed for comparison in these figures. Since the load cells, LC2 and LC3 in Fig. 3(c), were found to fail in measuring the force, only the forces measured by the other load cells were used. Therefore, the histories derived from load cells do not match those obtained from the accelerometers, but follow very closely the trend given by the accelerometers. It is worthwhile to note that, in Fig. 7(b), the history of shear obtained from the load cells in the *Y* direction appears to be almost identical in the negative side to that derived from the accelerometers. For torsion, the histories derived from the load cells occupy approximately 70% to 80% of those derived from accelerometers, whereas the overturning moments derived from the load cells appear to be almost equivalent to the values obtained from measured

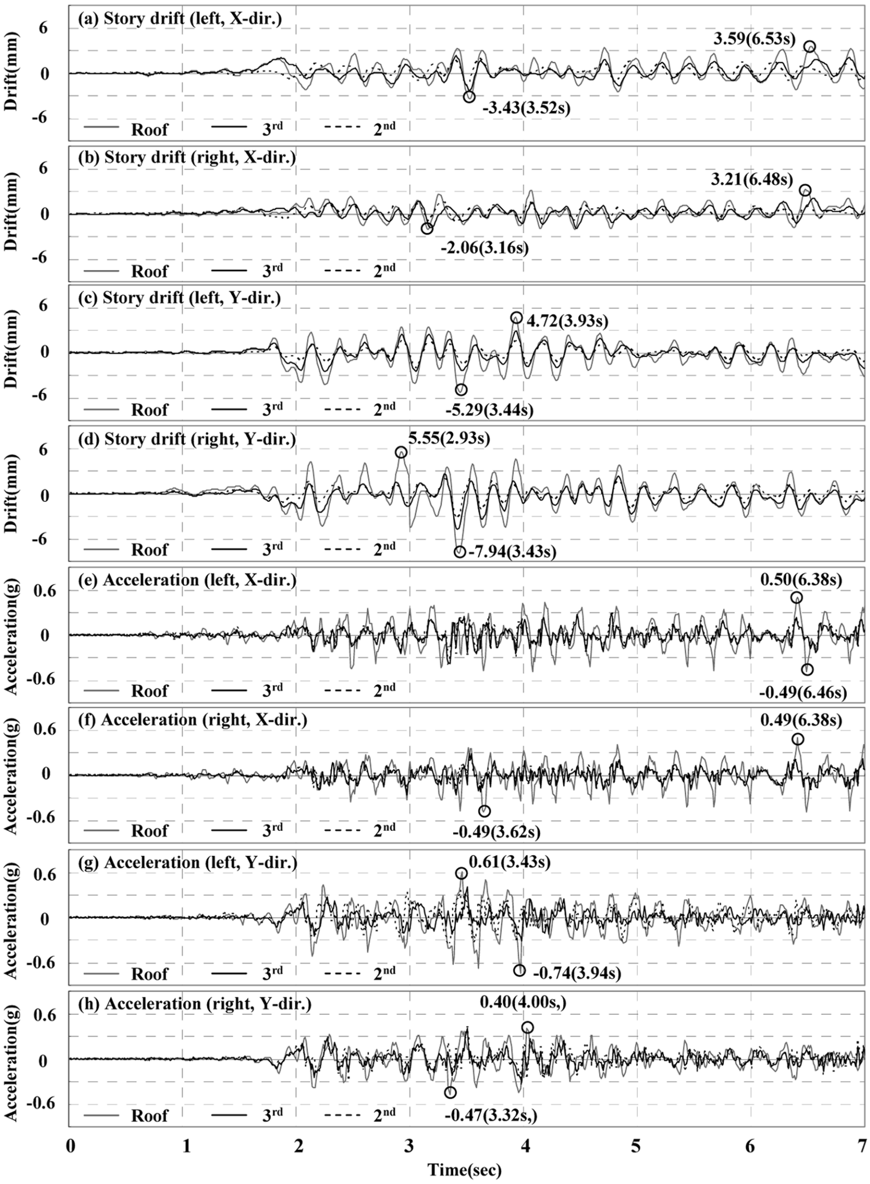

Fig. 6 Story drifts and accelerations: 0.154*XY*

horizontal accelerations. In spite of the shortcomings of the data obtained from load cells, since the information provided by the load cells was found to be still useful, it will be utilized wherever appropriate for the analysis of the experimental results hereafter.

The hysteretic curves between the base shear and the first story drift and between the torsion moment and torsion deformations are given in Fig. 10 and Fig. 11 for the levels of intensity of 0.070 g and 0.154 g, respectively. The model behaved linear-elastically under the 0.070*X* test. A very low level of inelastic response in the hysteresis between the base shear and drift in the *X* direction and significant energy dissipation in the torsion response can be observed whereas the

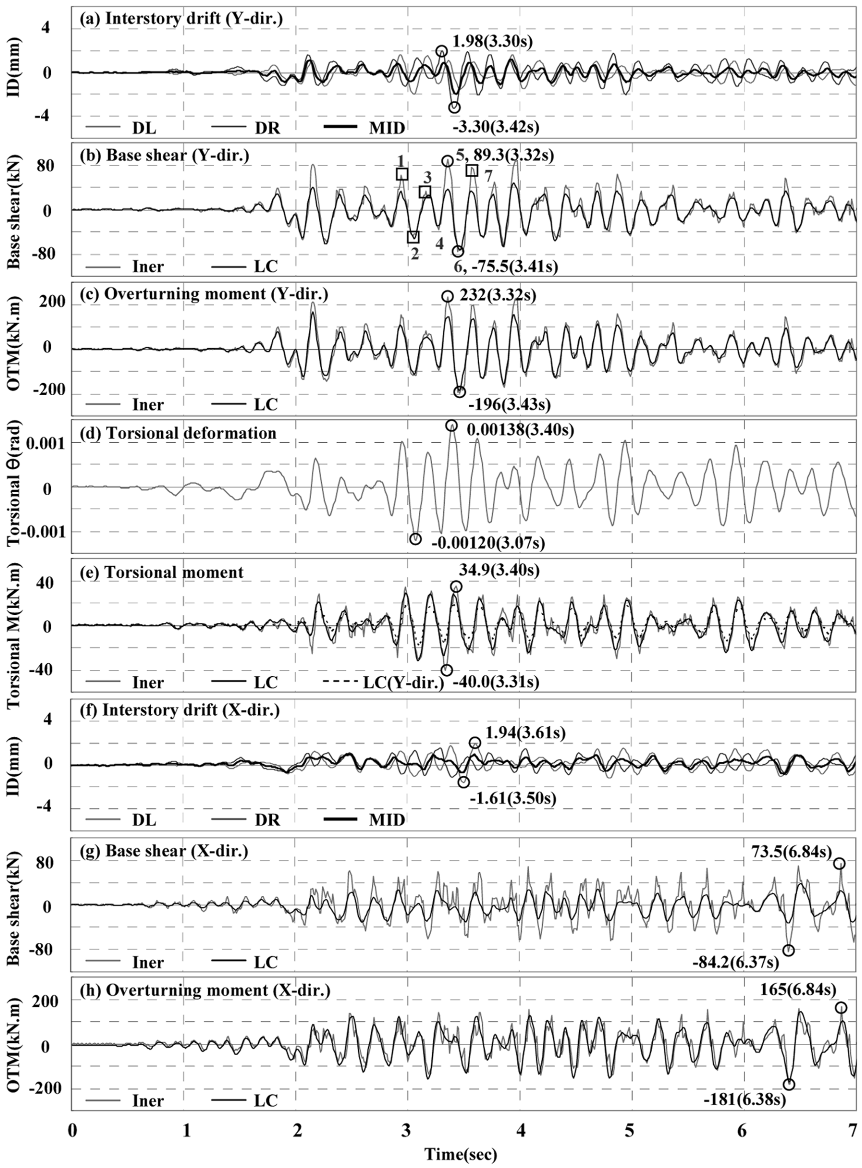

Fig. 7 Time histories of responses at first story under 0.154*XY* (See Fig. 3(c) for DL and DR, MID = 1/2 (DL + DR))

shear hysteresis in the *Y* direction shows a complete elastic behavior under the 0.070*XY* test, as shown in Fig. 10. Significant inelastic behaviors can be noticed in the shear response in the *X* direction and in the torsion response under the 0.154*X* test. Inelastic responses in the *Y* direction and torsion are observed under the 0.154*XY* test in Fig. 11, even though the amount of energy dissipation appears to be somewhat low.

The maximum values of base shears and drifts in the *X* and *Y* directions and the torsion moment and torsion deformation are shown for each test in the sequence of increasing intensity in Fig. 12.

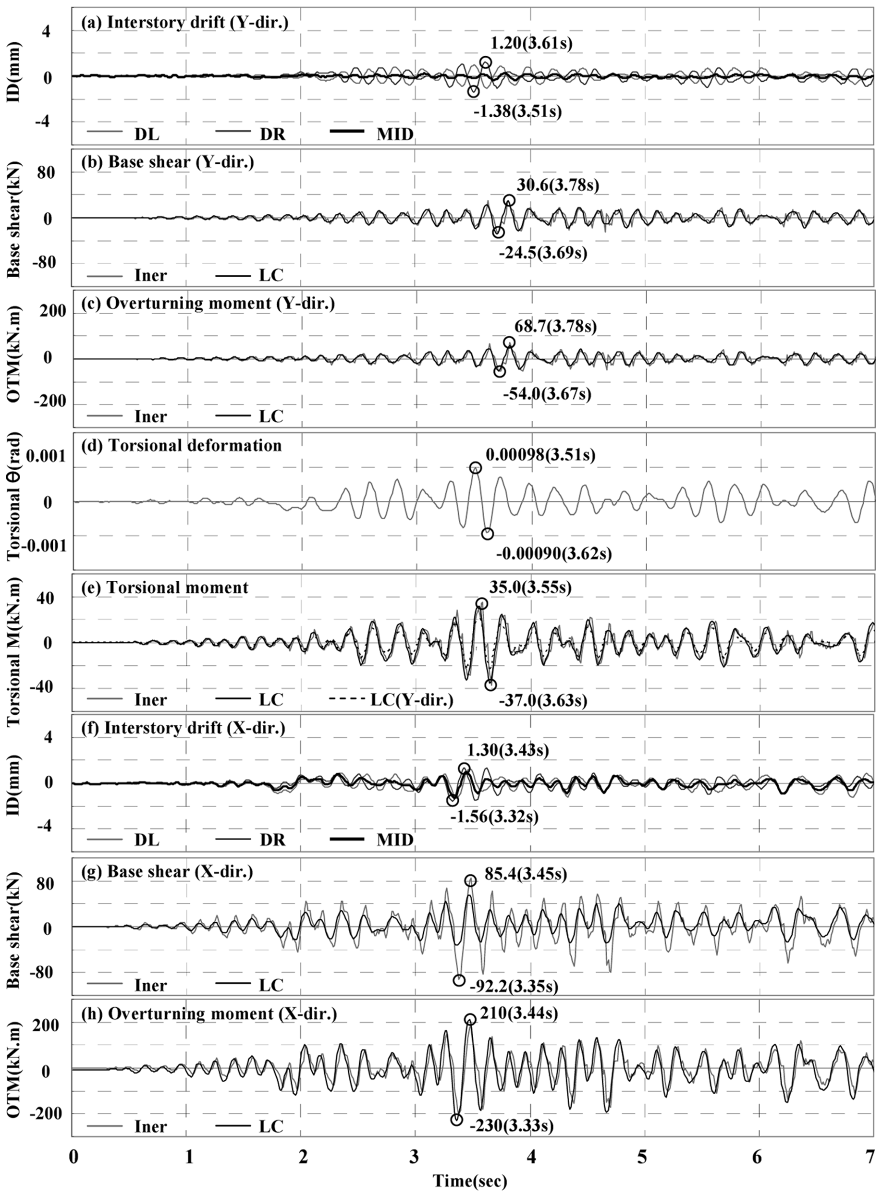

Fig. 8 Time histories of responses at first story under 0.154*X* (See Fig. 3(c) for DL and DR, MID = 1/2 (DL + DR))

The *X* series excitations caused a similar level of responses in the *X* direction in the base shear and the IDR at the first story when compared with the *XY* series.

However, the maximum values of base shear and IDR in the *Y* direction in the tests of the *X* series were much smaller than in those of the *XY* series. The maximum values of base shear in the *Y* direction keep increasing up to 109 kN in base shear and 0.48% in the IDR under the 0.187*XY* test. On the contrary, the maximum values of torsion moment and torsion deformation remain almost constant after 0.070*XY* test, at the levels of 35.9 kNm and 0.00115 radian, respectively. Also,

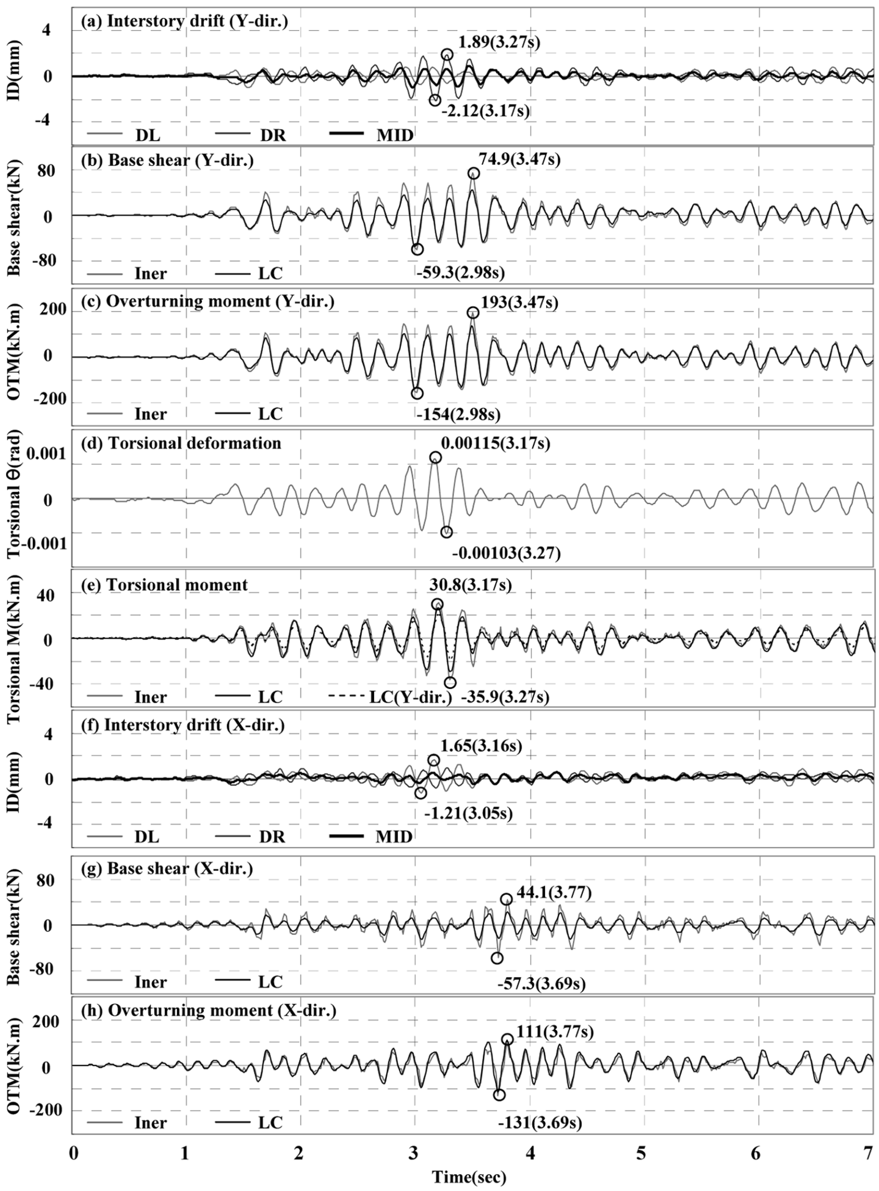

Fig. 9 Time histories of responses at first story under 0.070*XY* (See Fig. 3(c) for DL and DR, MID = 1/2 (DL + DR))

the maximum values of base shear in the *X* direction reached about 92 kN for both levels of 0.154 g and 0.187g with the IDR being approximately with 0.3%.

Inter-story drift ratios (IDR's): The vertical distributions of IDR in Fig. 13 reveal that the largest deformations are concentrated in the first story. The IDR's at the second story on the right side in the *X* direction are much smaller than those on the left side, which are almost at the level equivalent to the first story. The largest IDR in the *X* direction reaches 0.33% with that in the *Y* direction being 0.56% under test 0.154*XY*. The response of base shear versus the first story drift in

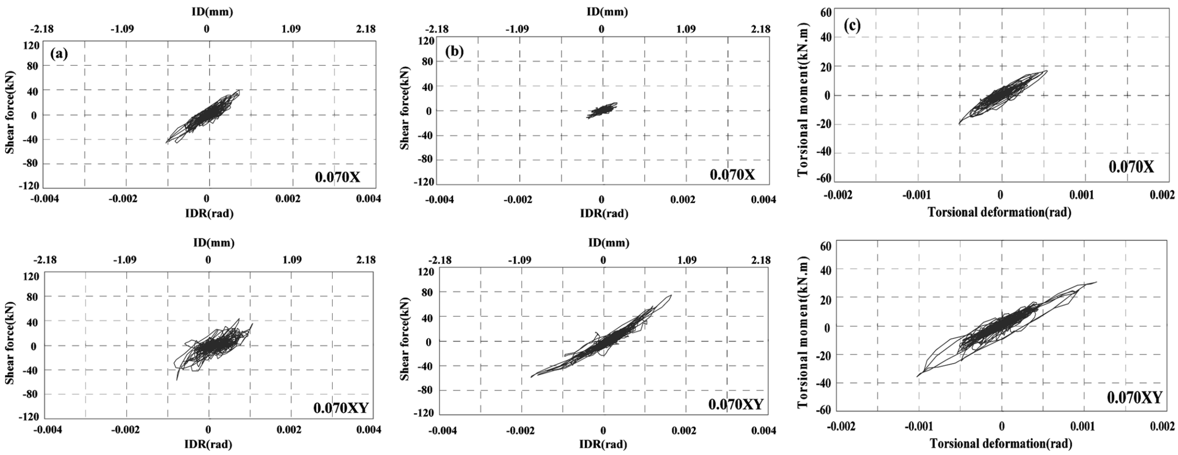

Fig. 10 Hysteretic curves under 0.070X and 0.070XY; (a) shear force versus IDR (X dir), (b) shear force versus IDR (Y dir), (c) Torsion moment versus Torsion deformation

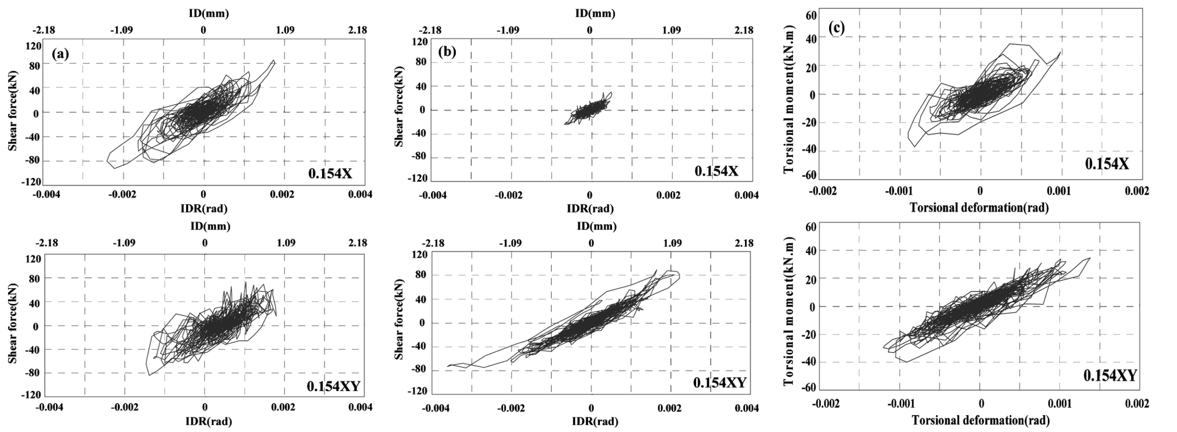

Fig. 11 Hysteretic curves under 0.154X and 0.154XY; (a) shear force versus IDR (X dir), (b) shear force versus IDR (Y dir), (c) Torsion moment versus Torsion deformation

the Y direction in Fig. 10(b) reveals that the structure remained in the elastic range reaching almost 0.2% IDR under the 0.070XY test, which is assumed to correspond to the earthquake with the return period of 50 years in Korea.

Comparison of responses among 0.154*XY*, 0.070*XY*, and 0.154*X*: The uni-directional excitations in the X-direction caused relatively low Y-directional drifts, and thereby low Y-directional base shear. The histories of torsion moment and torsion deformation are similar in shape and magnitude regardless of the intensity and directions of excitations, and influenced greatly the X- and Y-directional drifts. Also, in any test, the torsion moment resisted by the Y-directional frames including Y-directional walls occupies approximately 60% of the total as shown by broken lines in Figs. 7(e), 8(e), and 9(e).

Uncoupling between translational and torsional motions: Since the time interval from 2.9 seconds to 3.7 seconds covers the largest base shears in the positive and negative Y directions in

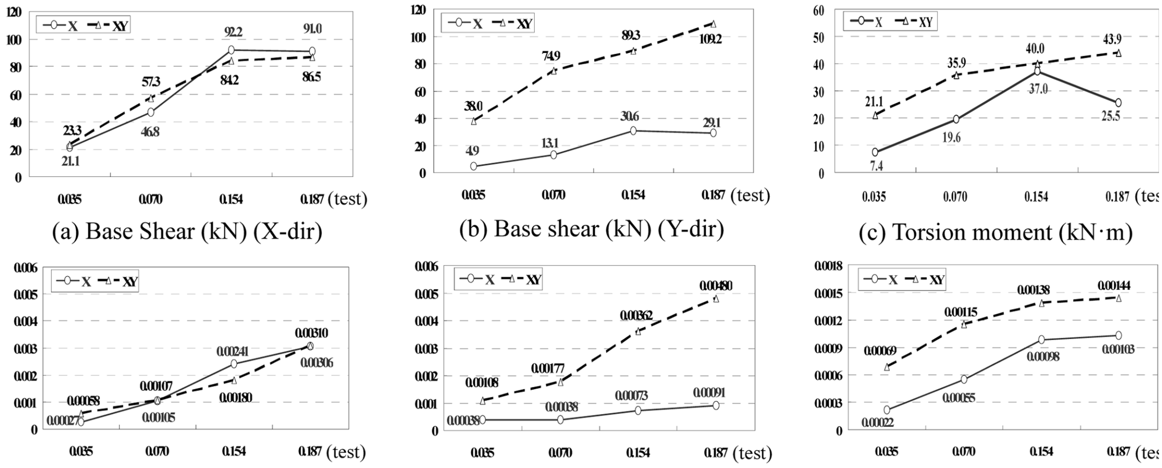

(a) Base Shear (kN) (X-dir) (b) Base shear (kN) (Y-dir) (c) Torsion moment (kN·m)
(d) IDR (rad) (X-dir) (e) IDR (rad) (Y-dir) (f) Torsion deformation (rad)

Fig. 12 Comparison responses between uni- and bi- directional excitations

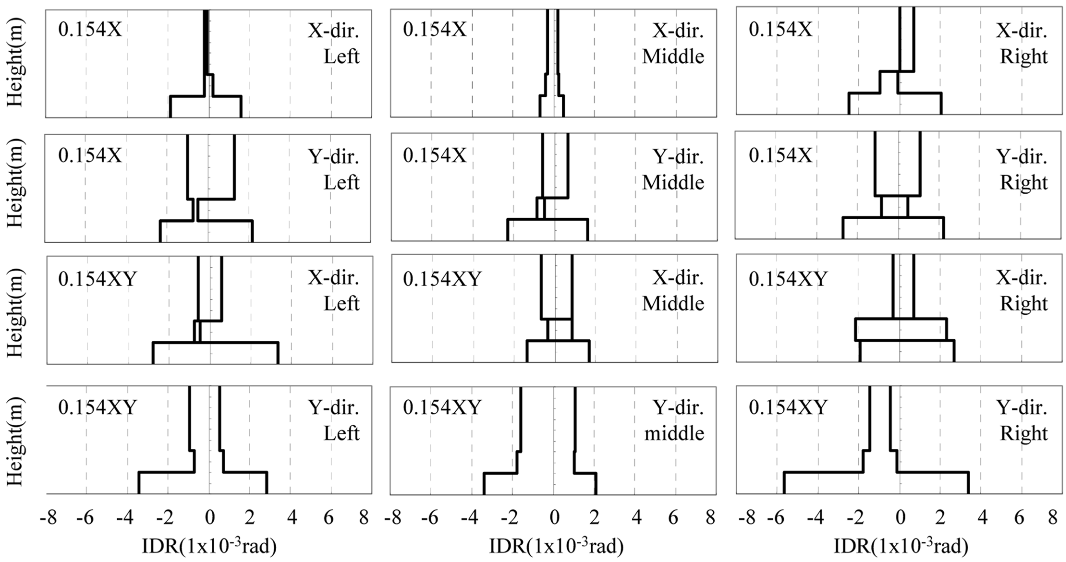

Fig. 13 Inter-story drift ratio at time of max. first story drift

Fig. 7(b), it is decided that the state of the base shear and first story drift with the state of torsion moment and torsion deformation will be traced in the hysteretic curves, in Fig. 14, by identifying the points corresponding to the points designated with the numbers of 1 to 7 as shown in Fig. 7(b). While most of the points are within the middle region in the *X*-direction shear in Fig. 14(a), indicating that the *X* directional motions are independent from those of the *Y* direction, the peak points, 5, 6, and 7 in Fig. 14(b), are near the peak points in torsion as shown in Fig. 14(c). It is interesting to note that the points 1, 2, 3, and 4 in Fig. 14(b) lie in the middle zone in Fig. 14(c). This means that the mode of translation in the *Y* direction does not coincide with the torsion mode even though the periods of both modes are close to each other.

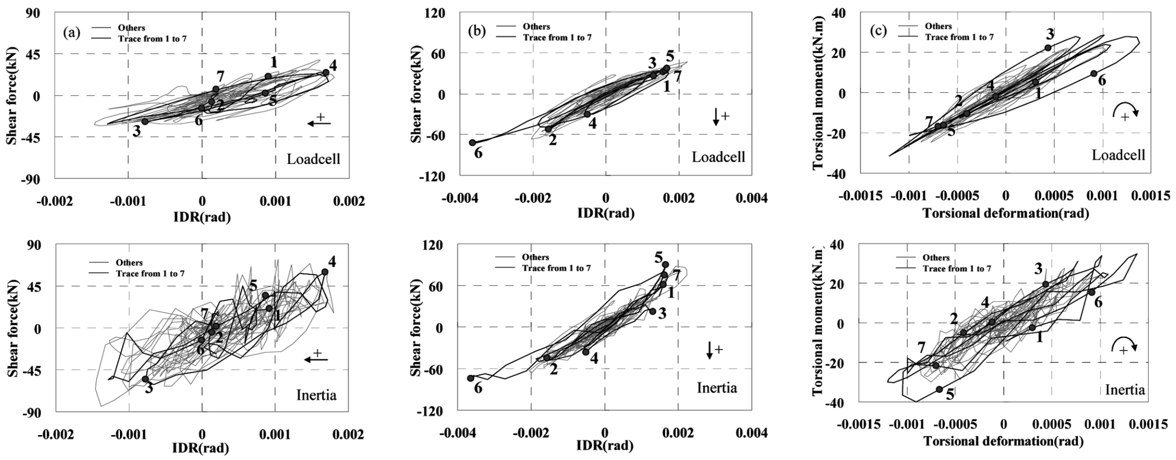

Fig. 14 Hysteretic curves of force versus deformation at first story under 0.154*XY*: (a) *X*-shear versus X-IDR, (b) *Y*-shear versus *Y*-IDR, (c) Torsion versus torsion deformation

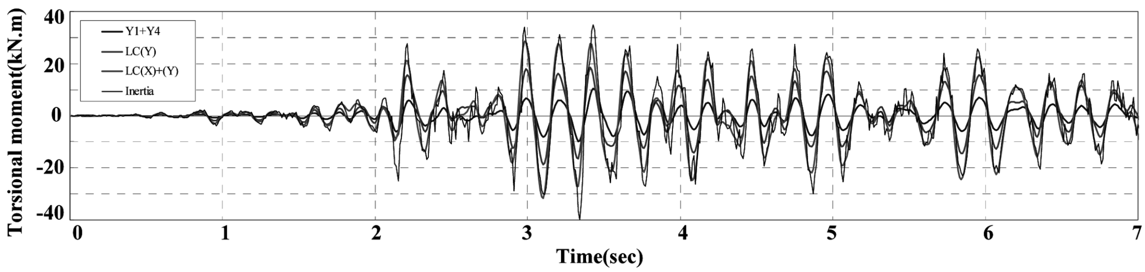

(a) Time history of torsion moment

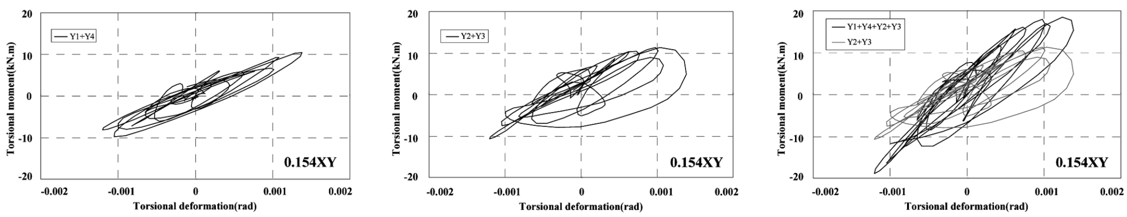

(b) Torsion contribution of Y1+Y4 frames and shear walls Y2+Y3 (2~4sec), 0.154XY

Fig. 15 Contribution of frames to torsion moment

Contribution of *X*- and *Y*-directional frames and walls to torsion: Under the unidirectional excitations as shown in Fig. 8, the transverse frames and walls played the role of restraining the torsion induced by the *X*-directional excitations, and, therefore, the base shears in the transverse direction was small in comparison with those in the excited direction. The contributions of *Y*-directional frames to the torsion moment under 0.154*XY* are given in Fig. 15(a). Most of the torsion measured through load cells originated from the *Y*-directional load cells. Fig. 15(b) compares the contributions of the outer frames Y1 + Y4 and the inner shear walls Y2 + Y3 to the torsion through the hysteresis curve of torsion versus torsion deformation. See Fig. 3(c) for the definition of frames Y1 to Y4. It can be seen in Fig. 15 that the torsion was distributed between the outer frames and core walls by the approximate ratio of 1:1.

4.2 Interaction between torsion and translational responses

This model shows a high degree of torsion irregularity. The topic of torsion has been an important issue for several decades among the researchers and engineers in the field of earthquake engineering (Rutenberg 1992, Del La LLera 1995, Paulay 2001) around the world.

Periods of fundamental modes: The results of Fast Fourier Transforms (FFT) of the time histories of base shears and torsion moment derived from inertia forces in Table 5 show that under test 0.154*XY* the first mode is the torsion mode (T_1 = 0.248 s) with the second mode (T_2 = 0.216 s) being the translational mode in the *Y* direction, and the third mode (T_3 = 0.160 s) being the translational mode in the *X* direction. It is interesting to note that the translational mode in the *Y* direction instead of in the *X* direction appears to be the second mode even though the two walls in the *Y* direction are stronger than the single wall in the *X* direction and the modal analysis have shown the translation mode in the *X* direction to be the second (Lee 2010). The reason for this unexpected result is not clear as yet and more study is needed in the future.

Correlation between torsion and translational responses: Though the torsion mode is not coupled with the second and third translational modes for this model, it will be worthwhile to investigate the relationships among the base shears in the *X* and *Y* directions and the torsion moments by using the interaction hysteretic diagrams (*X*-shear versus *Y*-shear, *X*-shear versus torsion, and *Y*-shear versus torsion) as shown in Fig. 16, where the 0.070*X* and 0.070*XY* tests represent the response of the model in the elastic range. In test 0.070*X*, the *X*-shear has some correlation with the torsion whereas the *Y*-shear does not. On the contrary, in test 0.070*XY*, the *Y*-shear manifests a clear correlation with the torsion while the *X*-shear is independent of the torsion. In test 0.154*X*, the phenomenon that is almost similar to test 0.070*X* can be observed with the range of diagrams expanded. However, in test 0.154*XY*, the correlations of *X*- and *Y*- shears with the torsion appear to differ significantly from those of the previous tests. That is, the directivity in the diagrams disappears, leading to a circular shape. For example, in the interaction diagram between the torsion and *Y*-shear for 0.154*XY* in Fig. 16(c), the traces starting from 3.38 s to 3.45 s are shown for both inertia force and load cell based cases. During the time interval from 3.38 s to 3.41 s, the *Y*-shear decreased from −18.3 kN to the minimum value of −75.5 kN with the torsion remaining almost constant, merely changing from 21.7 kNm to the maximum value of 32.7 kNm. In addition, during the time interval of 3.41 s to 3.45 s, the torsion decreased from 32.7 kNm to 1.36 kNm while the value of *Y*-shear changed only from −75.5 kN to −67.7 kN. This high inter-independence between shear and torsion can be attributed to the rapid variation in the shear forces in the *Y*-directional walls within a short duration and with a small change in lateral drifts as shown in the snap shots of Fig. 17.

Table 5 Natural periods obtained through FFT of time histories of inertia forces (unit: sec)

Test	0.035*X*	0.035*XY*	0.070*X*	0.070*XY*	0.154*X*	0.154*XY*	0.187*X*	0.187*XY*
V_x	0.160	0.160	0.160	0.160	0.160	0.160	0.169	0.160
V_y	0.168	0.193	0.178	0.202	0.190	0.216	0.190	0.214
Torsion	0.219	0.229	0.226	0.248	0.233	0.248	0.245	0.248

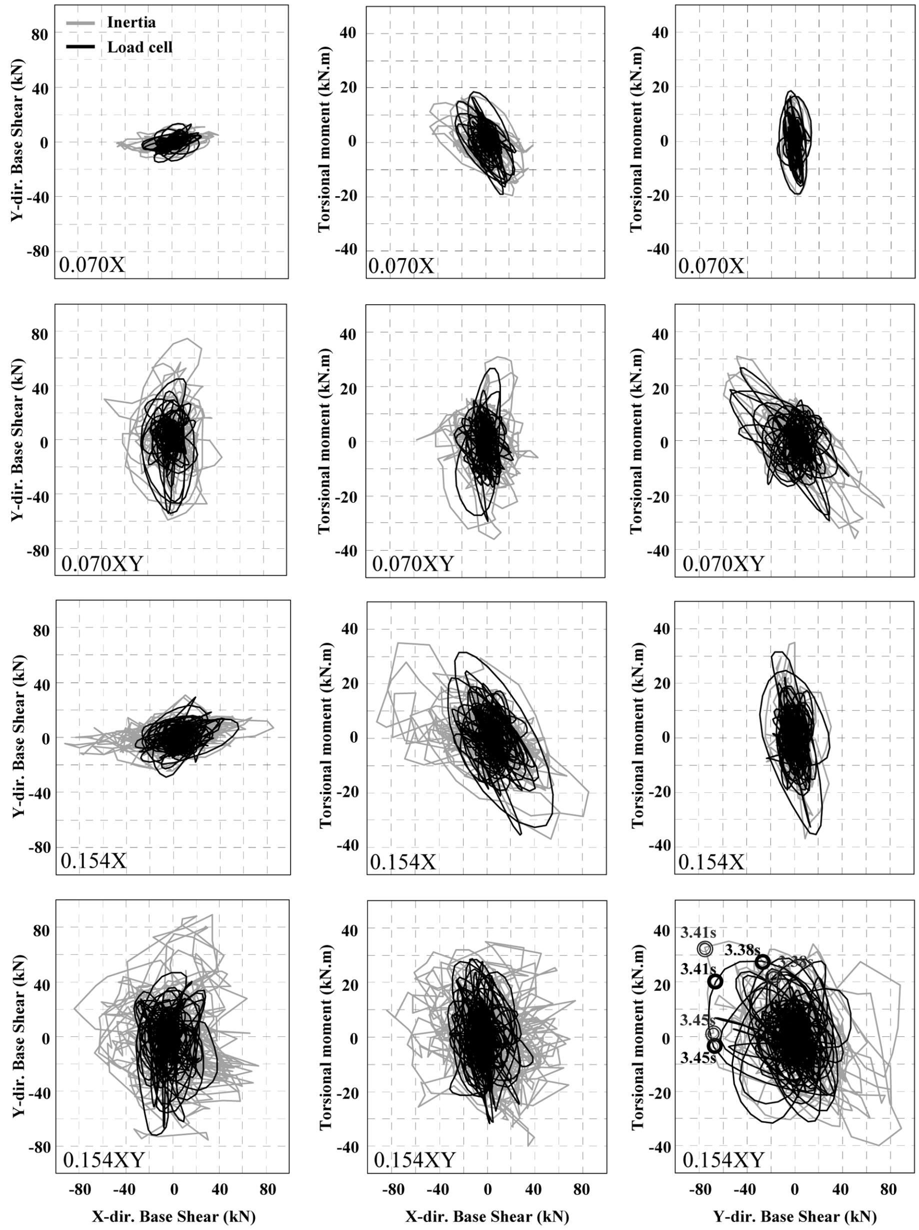

(a) Shear force(X) - Shear force(Y)
(b) Shear force(X) - Torsion moment
(c) Shear force(Y) - Torsion moment

Fig. 16 Correlations among base shear (V_X and V_Y) and base torsion under uni-directional (0.070*X*, 0.154*X*) and bi-directional (0.070*XY*, 0.154*XY*) excitations

4.3 Local responses

Minor hair cracks were found only on column C4 and wall C3-C7 after test 0.187*XY* as shown in Fig. 18, where it is seen that column C4 was mainly subjected to flexural and axial deformations.

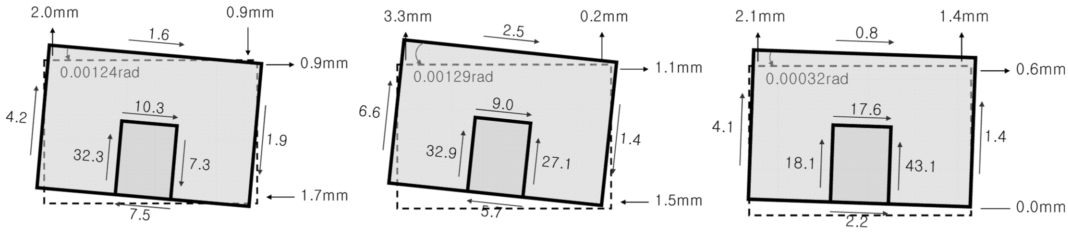

3.38 sec	3.41 sec	3.45 sec
Inertia (23.2, -18.3, 21.7)	Inertia (30.7, -75.5, 32.7)	Inertia (-32.8, -67.7, -1.36)
LC (-4.3, -27.3, 27.7)	LC (-5.8, -65.3, 20.0)	LC (-20.7,-66.7, -3.78)

(X-shear, Y-shear, Torsion)

Fig. 17 Snap shots (0.154*XY*, unit: kN, kN, kNm)

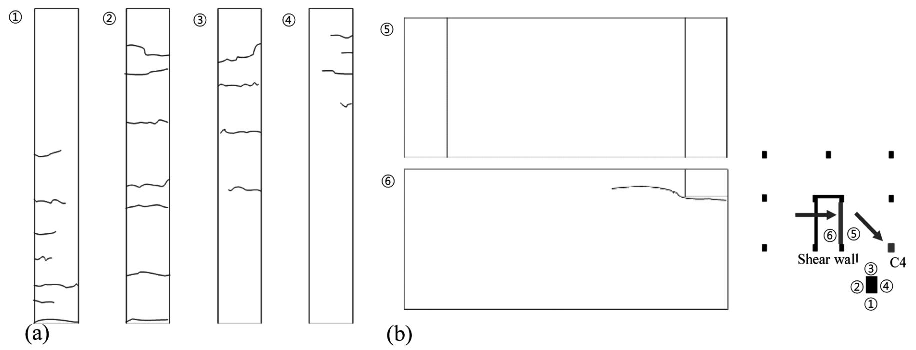

Fig. 18 Hair cracks after 0.187*XY*; (a) Column C4 and (b) Wall C3-C7

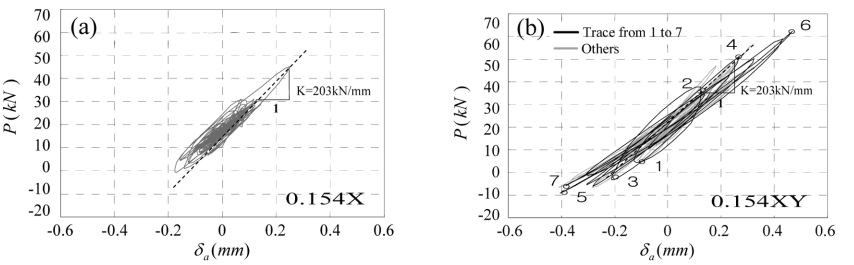

Fig. 19 Axial force (P) versus deformation (δ_a) of column C9; (a) 0.154X and (b) 0.154XY

However, the most severe lateral drift occurred at the corner column, C9, as shown in Figs. 7(a) and (f). The unique wall in the X direction exhibited the inelastic response under 0.154X and 0.154XY tests. The walls in the Y direction also showed inelastic responses under 0.154XY test. Detailed behaviors of these critical members are discussed in this section.

The relationships between the axial force and axial deformation in column C9 under 0.154X and 0.154XY tests are given with the stiffness estimated by using the Young's modulus of elasticity for concrete in Fig. 19. The interaction hysteretic diagrams among the axial force, the first story drifts and shear forces in the X and Y directions for C9 are shown in Fig. 20. The relation between shear force and first story drift in the Y direction in Fig. 20(e) indicates the bias in lateral shear resistance

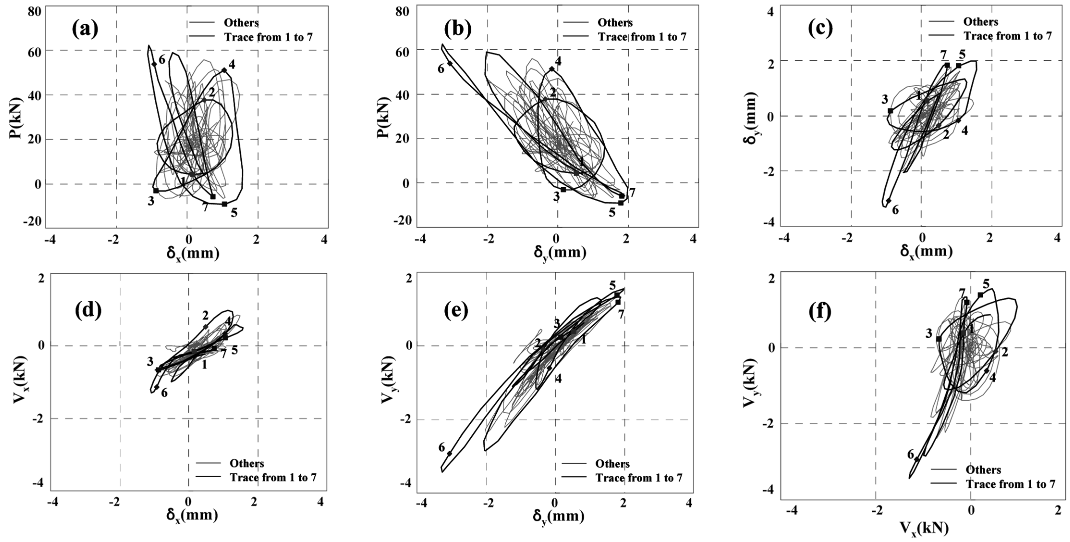

Fig. 20 Behavior of column C9 under 0.154 *XY*; (a) P versus δ_x (b) P versus δ_y (c) δ_x versus δ_y (d) V_x versus δ_x (e) V_y versus δ_y (f) V_x versus V_y

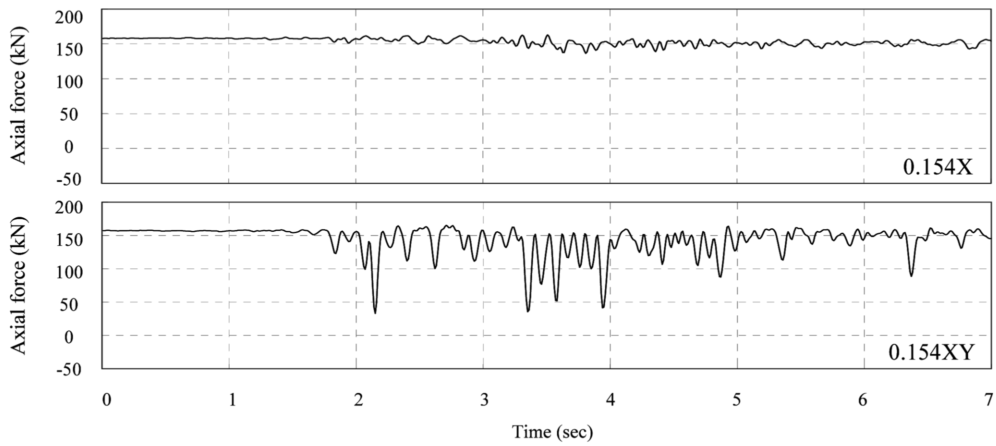

Fig. 21 Time histories of axial forces in wall C6-C7 under uni-directional and bi-directional excitations: 0.154*X* and 0.154*XY*

due to acting axial forces as shown in Fig. 20(b). In other words, the highest compressive force at point 6 caused the highest shear resistance and stiffness with the lowest shear resistance and stiffness at the lowest compressive (or highest tensile) axial force at points, 5 and 7.

The time histories of axial forces in wall C6-C7 under the unidirectional (0.154*X*) and bidirectional (0.154*XY*) excitations in Fig. 21 clearly show that the wall experienced the rocking phenomenon in the *Y* direction under 0.154*XY* test, which caused abrupt reduction of compressive axial force, whereas very low fluctuation of axial force occurred under 0.154*X* test. The interaction hysteretic diagrams between the axial force and flexural moment under 0.154*X* and 0.154*XY* tests with the capacity diagram denoted by the dotted lines in Fig. 22(a) reveal that wall C6-C7 only reached the flexural yielding for a short moment at around 3.33 sec under 0.154*X* test. The abrupt

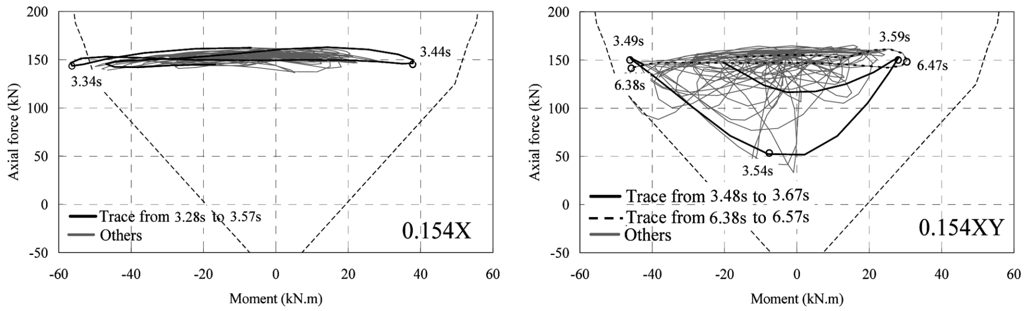

(a) Axial force versus bending moment

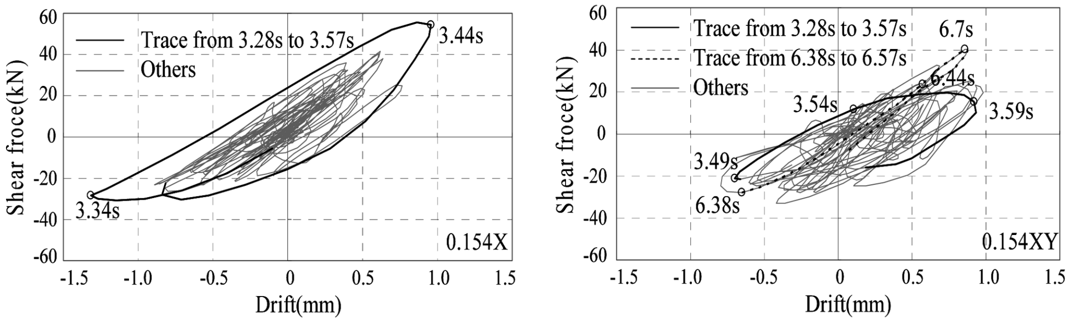

(b) Shear force versus drift at first story

Fig. 22 Behavior of wall (C6-C7)

reduction of axial compressive force caused reduction in the lateral resistance and stiffness under 0.154*XY* test when compared with those under 0.154*X* test as shown in Fig. 22(b).

5. Evaluation of seismic performance of the model according to KBC 2005 (IBC 2000) and FEMA 356

Evaluation on validity of KBC2005: The estimate of the building period using the empirical equation for the other structures as defined in KBC 2005 (IBC 2000), 0.156 s, appears to be reasonable in comparison to the periods of the second and third translational modes, 0.216 s (or sometimes 0.190 s) and 0.160 s, respectively. The values of maximum base shear normalized with respect to the effective weight are superposed on the design spectrum (R = 3, I_E = 1.0) and the elastic design spectrum (R = 1, I_E = 1.0) in Fig. 5(b) where it can be seen that the points of test results reside between the two spectra. The over strength factor of this model is about 2 with respect to the design spectrum (R = 3, I = 1.0), even though this building structure was not designed against earthquakes. The ratios of $\delta_{max}/\delta_{avg}$ (1.41 in X and 2.34 in Y direction) used in checking the criteria of torsion irregularity in KBC 2005 (IBC 2000) in Table.1 are verified to be reasonable with the test results: under test 0.070*XY* representing elastic responses, the ratios of $\delta_{max}/\delta_{avg}$ in the X direction were 1.50 and 1.66 at t = 3.04 s and 3.15 s, respectively, while those in the Y direction were 2.86 and 3.02, at t = 3.17 s and 3.28 s, respectively, as shown in Figs. 9(f) and (a). Also, the estimate of stiffness irregularity (0.63 in *X*-dir and 0.66 in *Y*-dir) can be verified with the test results shown in the IDR envelope at the time of maximum first story IDR in Fig. 13. Fig. 23 compares

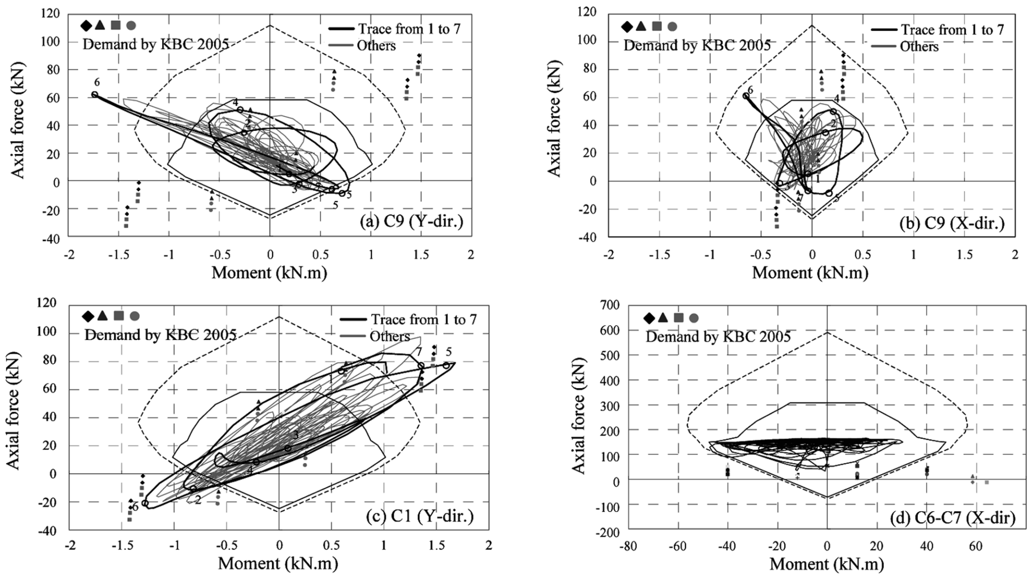

Fig. 23 Comparison of supply and demand by KBC 2005 (IBC 2000) and test results for columns C9, C1, and wall (C6-C7) under 0.154XY

the demands according to KBC 2005 (IBC 2000) denoted by markers and the supplied design strength and capacity through the P-M interaction diagrams as presented by solid and dotted lines, respectively, for critical members in the ground story, columns C9 and C1, and wall C6-C7. The over strength factor of 3.0 was used for the estimation of the demand according to KBC 2005. It can be noted that the demands by KBC 2005 far exceed the supplied strengths, and that the structure would therefore be unacceptable if KBC 2005 (IBC 2000) were used for safety judgment. Now, the hysteresis of P versus $V_y h$ under 0.154XY test is superposed with the P-M_y interaction capacity diagram for columns, C1 and C9 and wall C6-C7 in Fig. 23. Although the hysteretic diagrams exceeded the capacity for columns C1 and C9 in the Y direction, the strength demand determined from test results has a low probability of exceeding the flexural moment capacity for the following reasons; the value of $V_y h$ means the sum of the top and bottom flexural moments of the column in the Y direction and the points of contra flexure generally lie in the middle third region of the column. The hysteresis of P versus $V_x h$ overlapped by P-M_x interaction diagram reveals that this column did not yield in the X direction. Though some of the demands of KBC 2005 (IBC 2000) are outside of the capacity diagram, the demands by test results of wall C6-C7 are all within the capacity diagram due to much higher gravity compression force than that predicted by analysis.

Assessment of performance according to FEMA356: To evaluate the demand and capacity of critical members, the capacity assessment models according to FEMA 356 are given for column C9, wall C6-C7, wall C2-C6, and wall C3-C7 with the corresponding hysteretic relations between the force and deformation in Fig. 24. The positive and negative yield strengths in the assessment model for column C9 were governed by flexural yielding and calculated by using the P-M interaction capacity diagram and the peak axial forces measured at point 5 (tension side) and point 6 (compression side). Though column C9 is classified as a nonconforming element by FEMA 356 due to the spacing of transverse reinforcement larger than d/3, this column is assumed to be conforming in this assessment model. It can be noted in Fig. 24(a) and (b) that column C9 did not experience

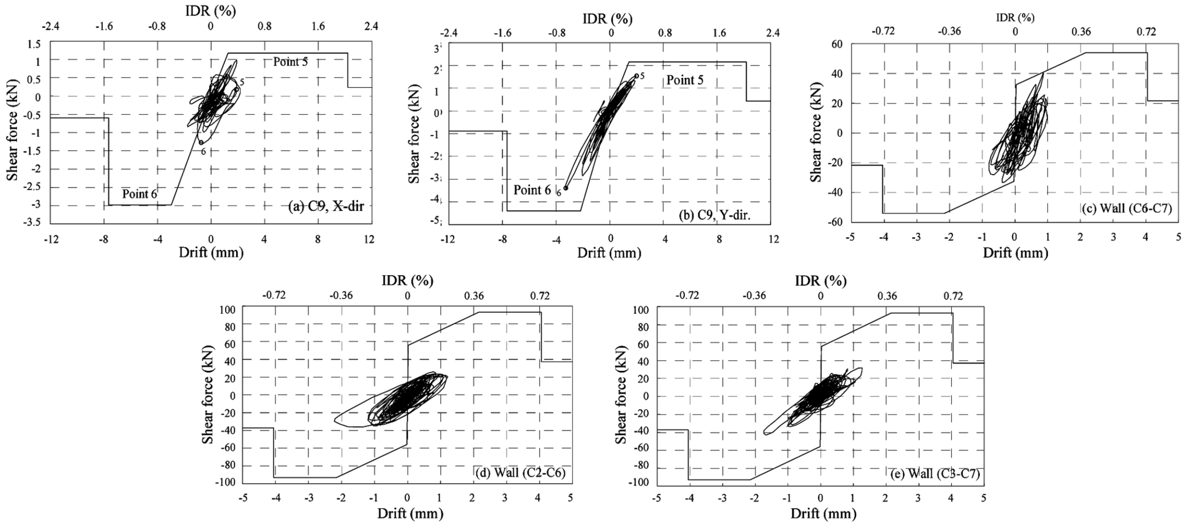

Fig. 24 Comparison of member responses with the assessment models by FEMA 356

yielding and the maximum drift ratio was approximately 0.7% under 0.154*XY*. The assessment model of walls was governed by the shear capacity as shown in Figs. 24(c) and (d). Wall C6-C7 had not yet yielded and its maximum drift ratio, 0.18%, is far less than the acceptable limit, 0.6%, for the life safety, specified by FEMA 356 and the deformation capacity of 0.72%. In Fig. 24(d), the deformation of wall C2-C6 has exceeded the yielding drift ratio, 0.36%, in a small amount and the measured shear force is much less than the yielding strength due to the malfunction of load cell, LC2. The maximum absolute drift ratio, 0.41%, is less than the limit of life safety, 0.6%, as prescribed by FEMA 356 and the deformation capacity of 0.72%. Similar result can be noticed in Fig. 24(e) for wall C3-C7.

6. Conclusions

The low-rise reinforced concrete residential buildings in the densely populated regions of the metropolitan cities in Korea usually use the ground story as parking spaces. This trend causes a high degree of irregularity with respect to the weak story, soft story, and torsion at the ground story. The research stated herein is addressed at the investigation and evaluation of the seismic responses of this type of building structures, which were not designed against earthquakes, through earthquake simulation tests with the intensity of earthquakes in low-to-moderate seismicity regions such as Korea. For this purpose, a 1:5 scale five-story RC building model was constructed and tested firstly by uni-directional and secondly by bi-directional shaking table excitations sequentially with increasing intensity. The following conclusions are drawn based on the analysis of test results:

(1) The model survived the design earthquake simulation with the PGA of 0.187 g, as specified in KBC 2005 (IBC 2000) without severe damage, even though it was not designed against earthquakes.

(2) Under the uni-directional excitations, the transverse frames and walls played the role of restraining the torsion induced by the excitations, and, therefore, the base shears in the transverse

direction was small in comparison with those in the excited direction. Most of the base shear in the transverse direction under bi-directional excitations was resisted by the core walls, while the torsion was distributed between the frames and core walls by the approximate ratio of 1:1 in the transverse direction.

(3) Under the bi-directional excitations, the two orthogonal translational modes acted independently. That is, there was no correlation between the two orthogonal translational modes. Nevertheless, the correlation of the torsion mode with one of the translational modes appears to be clear when the responses are within the elastic range and one of the translational modes is predominant over the other such as with the case of uni-directional excitations or with the case where the excitations in the Y direction are significantly more intense than those in the X direction. However, as the intensity of the bi-directional excitations increased, thereby causing large excursions into the inelastic range, this correlation disappeared. The maximum torsion moment and torsion deformation remained almost constant regardless of the excursions into the inelastic region in the X and/or Y directions.

(4) Under the bi-directional excitations, a high degree of rocking phenomena and the bi-directional overturning moments induced large variations in the axial forces in the corner columns and walls. The lateral resistance and stiffness of columns were greatly affected by the variation of axial forces acting on these columns. That is, the high compressive axial force caused high lateral resistance and stiffness whereas the low compressive or tensile force significantly reduced the lateral resistance and stiffness. The same phenomena were found in the walls.

(5) The seismic evaluation of the building model according to KBC 2005 (IBC 2000) suggests that this model would fail under the design earthquake, thus contradicting the test results. The main reason for this contradiction is attributed to the overly high over-strength factor of 3. It would be reasonable to reduce the over-strength factor from 3 to 2 and to apply this factor only to the axial force with the exception of the shear and flexural moments. The seismic assessment models provided by FEMA 356 appear to be reasonable when compared with the test results. The responses of the critical columns and walls are deemed to be within the allowable limits of Life Safety as specified by FEMA 356 under the design earthquake.

Acknowledgments

The research presented herein was supported by the National Research Foundation of Korea through the contract No. 2009-0083626. The writing of this paper was supported by Korea University through the sabbatical leave granted to the first author during the period from March 1 to August 31 in 2010.

Reference

American Society of Civil Engineers (2006), ASCE/SEI 41-06, *Seismic Rehabilitation of Existing Building*, Reston, VA.

Architectural Institute of Korea (2005), *Korean Building Code (KBC2005)*, Seoul, Korea. (in Korean)

Bousias, S.N., Fardis, M.N., Spathis, A.L. and Kosmopoulos, A.J. (2007), "Pseudo-dynamic response of torsionally unbalanced two storey test structure", *Earthq. Eng. Struct. D.*, **36**(8), 1065-1087.

Bracci, J.M., Reinhorn, A.M. and Mander, J.B. (1995), "Seismic resistance of reinforced concrete frame structures designed for gravity loads: performance of structural system", *ACI Struct. J.*, **92**(5), 597-609.

Del La LLera, J.C. and Chopra, A.K. (1995), "Understanding the inelastic seismic behavior of asymmetric-plan buildings", *Earthq. Eng. Struct. D.*, **24**, 549-572.

FEMA (2000), "Pre-standard and commentary for the seismic rehabilitation of buildings", Rep. No. FEMA-356, Federal Emergency Management Agency, Washington, D.C.

Fukuta, T., Kabeyasawa, T., Kuramoto, H. and Sanada, Y. (2001), "Shaking table tests and design analysis of a wall frame structure with soft first story", *Proceedings of the 4th International Symposium on Earthquake Engineering for the Moderate Seismicity Regions*, Seoul, Korea.

Harris, H.G. and Sabnis, G.M. (1999), *Structural Modeling and Experimental Techniques*, CRC Press, Boca Raton, FL.

Hashemi, A. and Mosalam, K.M. (2006), "Shake table experiment on reinforced concrete structure containing masonry infill wall", *Earthq. Eng. Struct. D.*, **35**(14), 1827-1852.

Hosoya, H., Abe, I., Kitagawa, Y. and Okada, T. (1995), "Shaking table tests of three dimensional scale models of reinforced concrete high rise frame structures with wall columns", *ACI Struct. J.,* **92**(6), 765-780.

International Code Council (2000), *International Building Code*, Falls church, VA.

Jung, D.W. (2010), "Earthquake simulation tests on a 1:5 scale piloti type low rise RC residential building model", Master Thesis, Korea University, Seoul, Korea. (in Korean)

Kang, T.H.K. (2004), "Shake table tests and analytical studies of reinforced concrete flat plate frames and post tensioned flat plate frames", Ph.D thesis, Univ. of California, Los Angeles.

Ko, D.W. and Lee, H.S. (2006), "Shaking table tests on a high-rise RC building model having torsional eccentricity in soft lower storeys", *Earthq. Eng. Struct. D.*, **35**, 1425-1451.

Lee, H.S. and Woo, S.W. (1998), *An Experimental Study on the Similitude in Structural Behaviors for Small-scale Modeling of Reinforced Concrete Structures,* Paper No. 308, 6th U.S. National Conference on Earthquake Engineering, Seattle, USA.

Lee, H.S. and Woo, S.W. (2002), "Effect of masonry infills on seismic performance of a 3 storey R/C frame with non seismic detailing", *Earthq. Eng. Struct. D.*, **31**(2), 353-378.

Lee, H.S. (2010), "Seismic performance evaluation and retrofit of piloti-type low-rise RC apartment buildings", Final Research Report, National Research Foundation of Korea, Korea. (in Korean)

Di Ludovico, M., Manfredi, G., Mola, E., Negro, P. and Prota, A. (2008), "Seismic behavior of a full scale RC structure retrofitted using GFRP laminates", *J. Struct. Eng.,* **134**(5), 810-821.

Paulay, T. (2001), "Some design principles relevant to torsional phenomena in ductile buildings", *J. Earthq. Eng.,* **5**(3), 273-308.

Rutenberg, A. (1992), "Nonlinear response of asymmetric building structures: a state of the art review", Nonlinear Seismic Analysis and Design of Reinforced Concrete Buildings, Eds. Fajfar, P. and Krawinkler, H., Elsevier Applied Science, Amsterdam.

Wu, C.L., Kuo, W.W., Yang, Y.S., Hwang, S.J., Elwood, K.J., Loh, C.H. and Moehle, J.P. (2009), "Collapse of nonductile concrete frame: shaking table tests", *Earthq. Eng. Struct. D.*, **38**, 205-224.

Zhao, B., Taucer, F. and Rossetto, T. (2009), "Field investigation on the performance of building structures during the 12 May 2008 Wenchuan earthquake in China", *Eng. Struct.*, **31**(8), 1707-1723.